Article

J. Braz. Chem. Soc., Vol. 23, No. 1, 163-170, 2012.
Printed in Brazil - ©2012 Sociedade Brasileira de Química
0103 - 5053 $6.00+0.00

Molecular Docking and Molecular Dynamic Studies of Semi-Synthetic Piperidine Alkaloids as Acetylcholinesterase Inhibitors

Amanda Danuello,[a] Nelilma C. Romeiro,[b] Guilherme M. Giesel,[c] Marcos Pivatto,[a] Claudio Viegas Jr.,[d] Hugo Verli,[c,e] Eliezer J. Barreiro,[b] Carlos A. M. Fraga,[b] Newton G. Castro[f] and Vanderlan S. Bolzani*[,a]

[a]Núcleo de Bioensaios, Biossíntese e Ecofisiologia de Produtos Naturais (NuBBE), Departamento de Química Orgânica, Instituto de Química, Universidade Estadual Paulista 'Julio de Mesquita Filho', CP 355, 14801-970 Araraquara-SP, Brazil

[b]Laboratório de Avaliação e Síntese de Substâncias Bioativas (LASSBio), Faculdade de Farmácia, Universidade Federal do Rio de Janeiro, CP 68023, 21944-910 Rio de Janeiro-RJ, Brazil

[c]Centro de Biotecnologia, Universidade Federal do Rio Grande do Sul, Av. Bento Gonçalves 9500, CP 15005, 91500-970 Porto Alegre-RS, Brazil

[d]Laboratório de Fitoquímica e Química Medicinal (LFQM), Departamento de Ciências Exatas, Universidade Federal de Alfenas, 37130-000 Alfenas-MG, Brazil

[e]Faculdade de Farmácia, Universidade Federal do Rio Grande do Sul, Av. Ipiranga 2752, 90610-000 Porto Alegre- RS, Brazil

[f]Departamento de Farmacologia Básica e Clínica, Instituto de Ciências Biomédicas, Universidade Federal do Rio de Janeiro, CCS Bloco J Sala J1-029, 21941-902 Rio de Janeiro-RJ, Brazil

A mistura dos derivados semissintéticos cloridrato da (–)-3-*O*-acetil-cassina e cloridrato da (–)-3-*O*-acetil-espectalina, preparada a partir da mistura dos alcalóides (–)-cassina e (–)-espectalina (4:1) obtida de *Senna spectabilis*, é um potente inibidor da acetilcolinesterase (AChE), assim justificando mais estudos moleculares. Neste sentido, estudos de *docking* e dinâmica moleculares foram conduzidos neste trabalho com o objetivo de adquirir uma compreensão mais profunda de todos os aspectos estruturais das moléculas cloridratos da (–)-3-O-acetil-cassina e (–)-3-O-acetil-espectalina, as quais diferem em seus potenciais inibidores de AChE. Os dois derivados em estudo apresentaram diversas interações com o sítio periférico aniônico dentro da cavidade catalítica de AChE de *Torpedo californica*. Entretanto, somente o composto majoritário (–)-3-*O*-acetil-cassina mostrou interação com a tríade catalítica de maneira significativa. As simulações de dinâmica molecular utilizando água como solvente foram importantes para compreender as interações hipotéticas entre cloridratos da (–)-3-O-acetil-cassina e (–)-3-O-acetil-espectalina com AChE. Os dados obtidos indicam que o composto (–)-3-*O*-acetil-cassina é o inibidor da enzima mais potente possivelmente devido às suas interações favoráveis com a proteína, com menor custo de dessolvatação. Estes resultados sugerem que o tamanho da cadeia lateral influencia no potencial inibitório das moléculas avaliadas e podem representar o ponto de partida para o desenvolvimento de novos derivados de (–)-3-*O*-acetil-cassina, objetivando a descoberta de inibidores de AChE mais eficazes.

The mixture of semi-synthetic derivatives (–)-3-*O*-acetyl-cassine hydrochloride and (–)-3-*O*-acetyl-spectaline hydrochloride, prepared from the mixture of natural alkaloids (–)-cassine and (–)-spectaline (4:1) isolated from *Senna spectabilis*, has been shown to be a potent acetylcholinesterase (AChE) inhibitor, thereby prompting further molecular studies. In this sense, docking and dynamic molecular studies were carried out in this work, aiming to acquire a deeper understanding about all the structural aspects of molecules (–)-3-*O*-acetyl-cassine and (–)-3-*O*-acetyl-spectaline hydrochlorides, which differ with respect to their AChE inhibitory potentials. Both molecules establish important interactions with the peripheral anionic site within the catalytic gorge of *Torpedo californica* AChE. However, only the major compound (–)-3-*O*-acetyl-cassine hydrochloride significantly interacts with the catalytic triad. Explicit-solvent molecular dynamic simulations were conducted in order to gain better understanding about the hypothetical interactions taking place between the semi-synthetic alkaloid molecules (–)-3-*O*-acetyl-cassine and (–)-3-*O*-acetyl-spectaline hydrochlorides and AChE. The data obtained in this study indicated that (–)-3-*O*-acetyl-cassine hydrochloride is the most potent inhibitor of AChE possibly due to the favorable interactions of this molecule with the target protein, with lower desolvation cost. These results suggested that the size of the side chain has an effect on the inhibitory potential of the evaluated molecules and may represent the starting point for the development of new derivatives of (–)-3-*O*-acetyl-cassine hydrochloride, with a view to the discovery of new effective AChE inhibitors.

Keywords: molecular docking, molecular dynamic, piperidine alkaloids, acetylcholinesterase inhibitors

*e-mail: bolzaniv@iq.unesp.br

Introduction

Alzheimer's disease (AD) is a late-onset neurodegenerative pathology that affects the memory, motor coordination, and cognition in a progressive, and eventually lethal, manner.[1-3] It has been postulated that at least some of the cognitive impairment experienced by AD patients results from deficient acetylcholine levels and consequent reduction in cholinergic neurotransmission. Consequently, the key approach employed in the development of drugs for use in the symptomatic treatment of AD has targeted the cholinergic deficit. Currently, only five drugs have received approval in the USA and Europe for therapeutic use in AD, namely tacrine (**1**; Cognex™),[4] donepezil (**2**; Aricept™),[5] rivastigmine (**3**; Excelon™),[6] galantamine (**4**; Reminyl™)[7] and memantine (**5**; Ebixa™)[8] (Figure 1). All of these compounds are acetylcholinesterase inhibitors (AChEIs),[4-7] with the single exception of **5**, which acts by blocking the *N*-methyl-D-aspartate (NMDA) glutamate receptors. It is apparent, therefore, that inhibition of acetylcholinesterase remains an important therapeutic strategy to the palliate cognitive deficit in AD.

The screening of numerous plant species that were typically selected based on their ethnobotanical data or report of their popular uses has been carried out in order to discover anticholinesterasic compounds with novel structural entities.[9-18] In this context, flowers, fruits, leaves and seeds from the ornamental plant *Senna spectabilis* (syn. *Cassia spectabilis*) (Fabaceae) have been reported to be sources of biologically rare piperidine alkaloids.[19] A deep analysis of the structural features of the naturally-occurring (–)-3-*O*-acetyl-spectaline (**6**) identified that part of this compound contains a molecular fragment similar to acetylcholine (ACh) (Figure 2). This has led to the preparation of several semi-synthetic derivatives, including (–)-3-*O*-acetyl-spectaline hydrochloride (**10**), which was prepared from natural piperidine (–)-spectaline (**8**). This derivative has been shown to display both *in vitro* (inhibitory concentration (IC_{50}) = 7.32 μM) and *in vivo* cholinergic activity during the spatial memory test (water maze).[20] Aiming to elucidate the mechanism of cholinesterase inhibition followed by this derivative, kinetic studies have revealed noncompetitive cholinesterase inhibition and central nervous selectivity with few peripheral side effects.[21]

Considering these results, compound **10** was selected as a prototype for further studies aiming to achieve a lead molecule. Additional scale-up fractionation of *S. spectabilis* and further isolation of the natural alkaloid **8** were monitored by electrospray ionization mass spectrometry (ESI-MS). This investigation revealed that the previously published piperidine alkaloids were in fact mixtures of two homologous piperidine alkaloid isomers (–)-cassine (**7**) and (–)-spectaline (**8**) at a ratio of 4:1, respectively (Figure 2).[22] So, the cholinesterase inhibition properties identified in that study were due to the mixture of (–)-3-*O*-acetyl-cassine hydrochloride (**9**) and **10** instead of being due to only the latter compound.

In spite of this problem, the main aim of this study was to investigate the binding patterns of the derivatives **9** and **10** with AChE and to verify the possible differences in their inhibition profiles. Molecular modeling studies of complexes formed between *Torpedo californica* acetylcholinesterase (*Tc*AChE) and the target semi-synthetic AChE inhibitors were accomplished by the application of flexible docking methodologies. The docking complexes were also submitted to explicit-solvent molecular dynamic (MD) simulations in water in order to gain dynamic understanding of the hypothetic interactions taking place between the molecules and AChE.

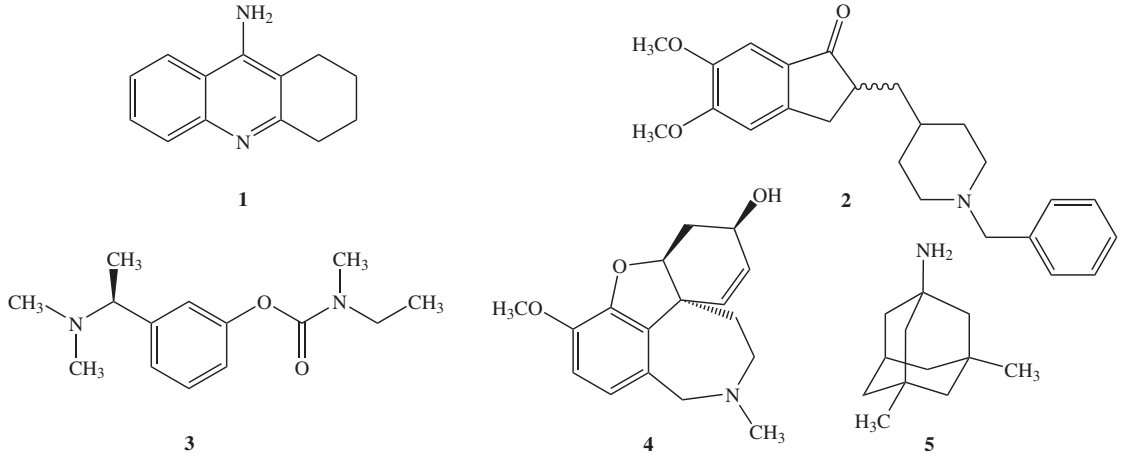

Figure 1. Marketed acetylcholinesterase inhibitors tacrine (**1**), donepezil (**2**), rivastigmine (**3**), galantamine (**4**) and NMDA/glutamate receptor blocker memantine (**5**).

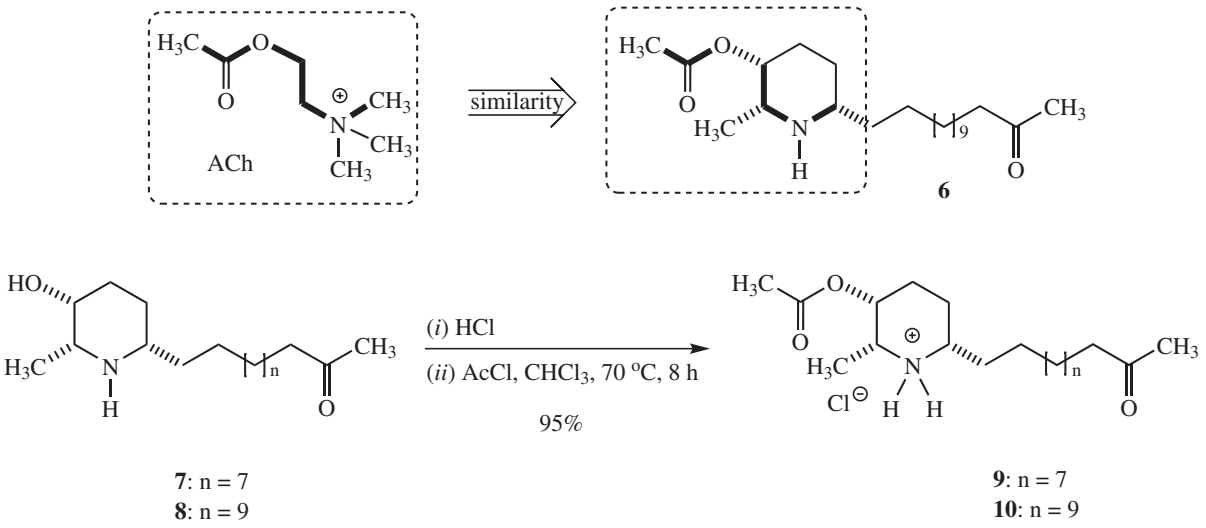

Figure 2. Molecular structures of (–)-3-*O*-acetyl-spectaline (**6**), (–)-cassine (**7**), (–)-spectaline (**8**), (–)-3-*O*-acetyl-cassine hydrochloride (**9**) and (–)-3-*O*-acetyl-spectaline hydrochloride (**10**).

A considerable amount of data related to the crystal structure of AChE and to various AChEI complexes is available.[23-25] With information, it is possible to apply molecular modeling methods to gain insight into the mechanism of action of the enzyme and to investigate the molecular determinants that modulate the molecular recognition of AChE inhibitors. Such knowledge can be exploited during the design of novel AChE inhibitors that might be more effective in the treatment of AD.[26-30]

Methodology

Molecular docking analyses

The accurate prediction of protein-ligand interaction geometries is essential for the success of the virtual-screening approaches employed during structure-based drug design. This procedure requires docking tools that are able to generate suitable conformations of a ligand within a protein-binding site and demands reliable energetic evaluations for the quality determination of the interaction. In this respect, the FlexX™ scoring function has been shown to be reliable in a variety of different cases, even when flexible ligands are concerned.[31] Thus, in the present study, docking with FlexE was performed using the default FlexX™ scoring function following the preparation of both the ligand and the protein.

Molecular docking analyses were accomplished by using the SYBYL 9 (Tripos Inc., St. Louis, MO, USA) version 7.2 software and the programs embedded therein. Formal charges were assigned, and the FlexX scoring function[31] was chosen for computation of the FlexE[32] docking poses.

Preparation of ligands for the docking studies

Ligand coordinates were generated using the sketcher tool embedded in the SYBYL software suite, and the correct atom types (including hybridization states) and bond categories were defined. Hydrogen atoms were subsequently added, Gasteiger-Hückel charges[33] were assigned to each atom, and the final structures were energy-minimized. Carboxylic acid groups were modeled in their anionic form, whereas amino groups were considered in their protonated form.

Preparation of protein structures for the docking studies

Three-dimensional crystal structures of *Tc*AChE complexed with huperzine, tacrine and donepezil were retrieved from the RCSB (Research Collaboratory for Structural Bioinformatics) protein data bank[34] under PDB IDs 1VOT, 1ACJ and 1EVE, respectively. The active site of *Tc*AChE was defined as the collection of residues within 15.0 Å of the bound inhibitor present in the reference structure 1ACJ. The bound inhibitors were not included in the docking runs.

For each structure, the description of an ensemble contains the definition of the protein atoms (via chain identifiers and hetero groups), the resolution of ambiguities in the PDB file (alternate location indicators etc.), the location of hydrogen atoms at the heteroatoms and the definition of the active site atoms. The first step in the generation of suitable protein structures for ensemble superimposition is the selection of one chain from the reference crystal structure (1ACJ). This process generally involves retention of chain A and deletion of other chains, if present.

Stepwise analysis and correction of the geometric parameters, including atom types, atom names, torsion angles, bump elimination and hydrogen addition, were carried out with the aid of the Biopolymer "protein preparation" tool embedded in the SYBYL software suite. The assignment of the hydrogen positions was based on default rules, except for the definition of the torsion angles at the hydroxyl groups of the amino acid residues serine, threonine and tyrosine, and the hydrogen position inside the histidine side chain. Charges were added according to the AmberF99 force field simulation.[35] The side-chains of lysine and arginine, and the carboxylate groups of aspartic and glutamic acids, were modeled in their ionized states. Water molecules contained in the PDB file were removed. After each docking run, thirty poses were saved in Mol2 files for further analysis.

Ligand topologies

The structure of each compound was submitted to the PRODRG Server,[36] and the initial geometries and crude topologies were retrieved on the basis of the best ranking docking poses previously obtained by flexible docking with FlexE. The employed atomic charges were derived from the Löwdin scheme and were obtained at the HF/6-31G** level using the program GAMESS[37] in an appropriated form for molecular dynamic calculations. Analyses were carried out using the GROMACS simulation suite[38] and the GROMOS96 force field, as previously reported.[39-41]

Molecular dynamic simulations

Three systems were submitted to molecular dynamic (MD) simulations: (*i*) uncomplexed AChE in solution, (*ii*) AChE complexed with **9** and (*iii*) AChE complexed with **10**. The GROMACS simulations suite and GROMOS96 force field were used by employing an MD protocol based on previous studies.[42] Briefly, these systems were solvated in triclinic boxes using periodic boundary conditions and the SPC water model.[43] Counter ions were added, so as to neutralize the charges of the systems. The LINCS method[44] was applied in order to constrain covalent bond lengths. This allowed for an integration step of 2 fs after an initial energy minimization step using the steepest descent algorithm. Electrostatic interactions were calculated with particle-mesh Ewald.[45] Temperature and pressure were kept constant by separately coupling protein, ligand, ions, and solvent to external temperature and pressure baths with constants of $\tau = 0.1$ and 0.5 ps, respectively.[46] The system was slowly heated from 50 to 310 K in steps of 5 ps, each one increasing the reference temperature by 50 K. After this thermalization, the reference temperature was maintained at 310 K. Interaction energies are presented as the sum of Coulomb and Lennard-Jones components over the entire MD trajectories. Ranked data were evaluated using Kruskal-Wallis one-way analysis of variance (ANOVA),[47] whereas pairwise multiple comparisons were assessed by the Tukey test.[48] Between-group comparisons were appraised with the Mann-Whitney rank sum test.[49,50]

Results and Discussion

Enzyme-inhibitor interactions at the bottom of the AChE gorge

The visual inspection of the ligand-*Tc*AChE complexes (Figures 3a-b) shows that the bottom of the active site gorge of AChE may be represented by amino acid residue Trp84. The evaluation of the best ranking docking poses obtained for **9** and **10** revealed that neither of these molecules was

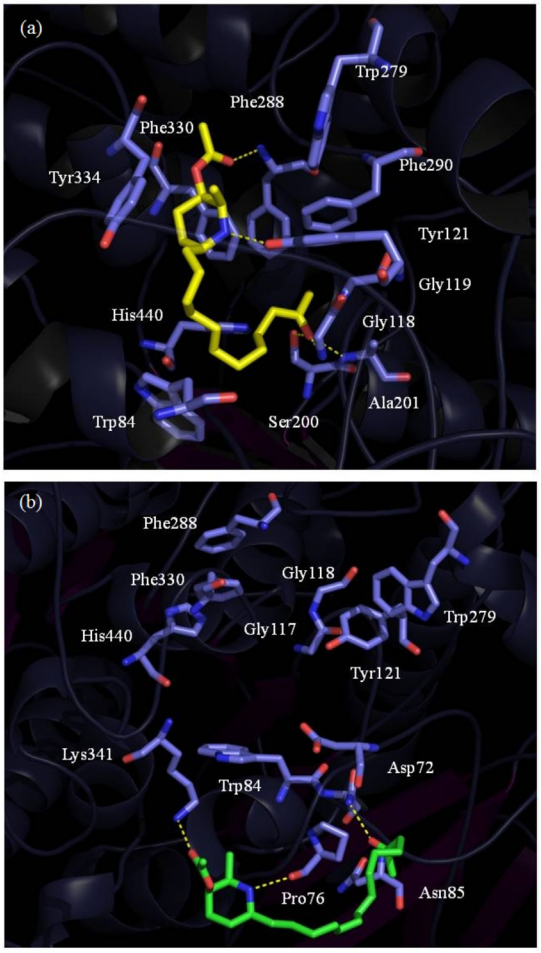

Figure 3. Top scored ligand-*Tc*AChE complexes obtained by flexible docking with FlexE for (a) **9** and (b) **10**. Non-polar hydrogen atoms were omitted for clarity. Only active site residues are shown. Hydrogen bonds are represented as green dashed lines.

able to penetrate deeply into the enzyme gorge. Presumably, this is a consequence of the volume of the long aliphatic side chains present in the two compounds. However, unlike its homologue **10**, acetyl hydrochloride derivative **9** was able to interact with one of the residues, hence forming the AChE catalytic triad (*i.e.*, Ser200, Glu327 and His440) through formation of a hydrogen bond linking the terminal oxygen atom of its acetyl group with Ser200.

Enzyme-inhibitor interactions in the middle of the AChE gorge

A constriction is located within the region considered to be the middle of the AChE active site gorge and is represented by amino acid residue Phe330 (Figures 3a-b). However, neither **9** nor **10** appear to interact with Phe330, although a binding site with **9** is located relatively close to this residue (Figure 3a).

Enzyme-inhibitor interactions at the entrance to the AChE gorge

Amino acid residues, including Tyr70, Tyr121 and Trp279, making up the peripheral anionic site of AChE are located close to the top of the active site gorge. The visual inspection of the top scoring pose of **9** reveals that the piperidine ring and the aromatic rings of Phe288 and Phe290 are within van der Waals contact distance (Figure 3a). Additionally, **9** is able to form hydrogen bonds with the –NH group of Phe288 via the ester function, with Gly118, Gly119 and Ala201 via the oxygen of the terminal acetyl group, and with Tyr121 via the hydrogen atom associated with the protonated amino group of the piperidine moiety (Figure 3a). In contrast, **10** can establish hydrogen bonds with Lys341 via the ester function, with Pro76 via the protonated nitrogen atom of the piperidine ring, and with Asn85 via the terminal acetyl group. It is noteworthy that, as compared to **9**, **10** binds to AChE in a perpendicular fashion, with an extended conformation (Figures 3a-b). Binding of compounds **9** and **10** to the peripheral anionic site of AChE is likely to generate a steric blockade of the enzyme gorge similar to that described for the anticholinesterasic drug donepezil, which presents analogous binding characteristics.[25]

Molecular dynamics stimulations

In order to obtain further information regarding the dynamics of AChE inhibition by **9** and **10**, complexes between the enzyme and the semi-synthetic derivatives were submitted to MD simulations in water. Figures 4a-b show the docking-obtained orientations of each compound superimposed on the respective 5 ns MD simulations, while Figure 4c depicts the 5 ns MD simulations of **9** and

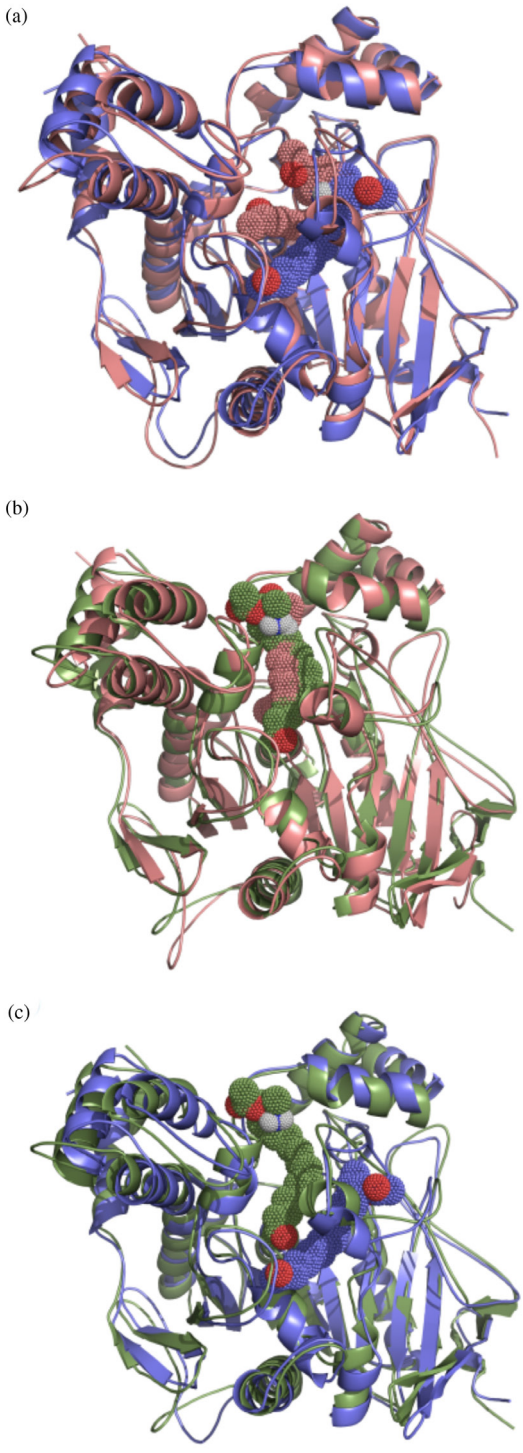

Figure 4. Superimposition of AChE complexed with **9** and **10**: (a) **9** in the docking-derived orientation (salmon) and after 5 ns MD (blue), (b) **10** in the docking-derived orientation (salmon) and after 5 ns MD (green) and (c) **9** (blue) and **10** (green) after 5 ns MD. Oxygen atoms are presented in red and polar hydrogen atoms in white.

10 superimposed one upon the other. Both compounds underwent significant reorientations in the simulated time scale, indicating an important role for the solvent with respect to the flexibility and stabilization of the complexes. However, such conformational accommodations did not appear to induce major modification in AChE dynamics or secondary structural elements (Supplementary Information, data available).

MD simulation revealed interactions between both molecules **9** and **10** and the amino acid residue Trp84 at the bottom of the enzyme gorge, although the binding energy of **9** with this residue (–7.7 ± 6.5 kJ mol^{-1}) was more favorable than that of **10** (–1.9 ± 2.6 kJ mol^{-1}) (Table 1). In the middle of the gorge, both **9** and **10** interacted with Trp432, which lies in a region close to the amino acid residue Phe330. At the top of the gorge, **9** exhibited binding with Tyr70 and Asp72, and exhibited a very favorable interaction with the latter residue with a binding energy of –13.7 ± 10.0 kJ mol^{-1}. Close to this region of the gorge, derivative **9** also interacted with Tyr121 and Ser122. Although **10** did not bind with these residues, it interacts with residues Gln74, Asp285, Ser286, Arg289, Tyr334 and Gly335 (Table 1).

Table 1. Interaction energies between **9** and **10** and the amino acid residues of *Tc*AChE, together with the interaction energies of the unbound molecules with the solvent (water)

Amino acid residues[a]	Energy / (kJ mol^{-1})[b]	
	Compound **9**	Compound **10**
Tyr70	–1.8 ± 1.5	0.0 ± 0.0
Asp72	–13.7 ± 10.0	0.0 ± 0.0
Gln74	0.0 ± 0.0	–3.6 ± 6.4
Trp84	–7.7 ± 6.5	–1.9 ± 2.6
Gly118	0.0 ± 0.0	0.0 ± 0.0
Tyr121	–5.0 ± 7.8	0.0 ± 0.0
Ser122	–2.1 ± 4.0	0.0 ± 0.0
Asp285	0.0 ± 0.0	–9.4 ± 8.1
Ser286	0.0 ± 0.0	–2.6 ± 2.5
Arg289	0.0 ± 0.0	–1.6 ± 2.5
Tyr334	0.0 ± 0.0	–4.0 ± 5.8
Gly335	0.0 ± 0.0	–2.0 ± 1.8
Trp432	–1.4 ± 2.9	–1.3 ± 1.9
ΔH_{AChE}	–34.0 ± 15.1[c]	–30.9 ± 17.7[c]
$\Delta H_{solvent}$	–77.7 ± 15.4[c]	–92.6 ± 16.5[c]

[a]Only the main interacting amino acid residues are shown; [b]fluctuation of each interaction along the performed simulations is presented in the Supplementary Information; [c]significant differences between values within a row (ANOVA; $p \leq 0.001$).

In view of the considerable flexibility shown by the AChE inhibitors, molecules **9** and **10** were also submitted to MD simulation on a 0.1 μs time scale in the presence of water but without the target protein (Figure 5). The data suggest that the increase in hydrophobicity of **10** as compared to **9** culminates in a greater entropic cost associated with the complexation of the former.

MD simulation of the AChE-inhibitor docking complexes AChE-9 and AChE-10 generated interaction energies of –34.0 ± 15.1 and –30.9 ± 17.7 kJ mol^{-1}, respectively (Table 1). The application of the Mann-Whitney rank sum test established that these values are statistically different ($p \leq 0.001$), a result that correlates with the observed differences in the biological activities of **9** and **10**. Similarly, the observed interaction energies between uncomplexed **9** and **10** and solvent water may be readily related to the enthalpic cost of desolvation associated with inhibition of AChE by these molecules. Therefore, the more active structure **9** may be seen as presenting a more favorable interaction with the target protein and as being held with lower intensity by the solvent. On the other hand, the less active compound **10** exhibits a less favorable interaction with the target receptor and a more intense interaction with the solvent.

Conclusions

The molecular modeling study described herein was carried out with the aim of elucidating the molecular basis of the differential AChE inhibition profiles of two semi-synthetic acetyl derivatives of the piperidine alkaloids (–)-cassine and (–)-spectaline isolated from *S. spectabilis*. Flexible docking revealed different binding conformations and interaction patterns for (–)-3-*O*-acetyl-cassine hydrochloride (**9**) and (–)-3-*O*-acetyl-spectaline hydrochloride (**10**) with respect to AChE, especially in the peripheral anionic site. Explicit-solvent molecular dynamic simulations in water revealed that the more active compound **9** presents a more favorable interaction with the target protein, as anticipated by flexible docking, at a lower desolvation cost. On the other hand, the less active compound **10** exhibits a less favorable interaction with the enzyme along with a more intense interaction with the solvent. These results emphasize the importance of the shorter side chain of **9** for a better interaction with AChE. This is due to reduced steric limitations to the entry of the inhibitor into the active site gorge. This finding will be able to guide the design of new derivatives of **9**, *e.g.*, via shortening of the side chain bearing different functionalities, aiming at the synthesis of anti-Alzheimer lead compounds based on natural products from our Brazilian biodiversity.

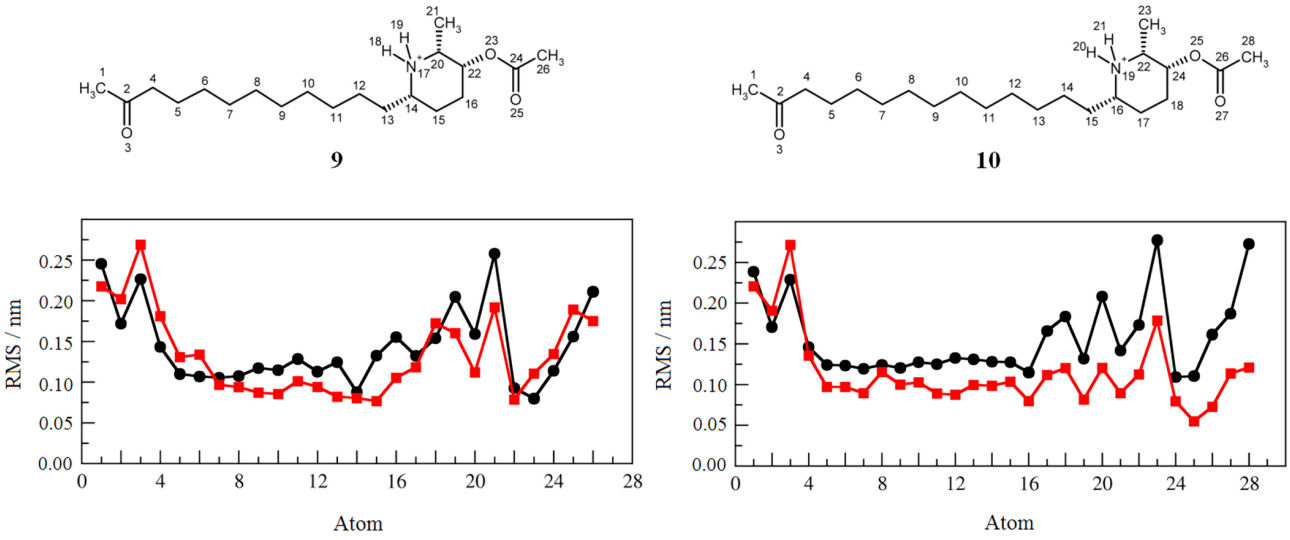

Figure 5. RMS fluctuation for **9** and **10** in uncomplexed (black curve) and complexed (red curve) forms.

Supplementary Information

Supplementary information (Figures S1-S7) are available free of charge at http://jbcs.org.br as a PDF file.

Acknowledgements

This research was supported by a grant (No. 03/02176-7) awarded to V. S. B. from Fundação de Amparo à Pesquisa do Estado de São Paulo (FAPESP) as part of the Biodiversity Virtual Institute Program (www.biota.org.br). A. D., H. V., E. J. B., C. A. M. F. and V. S. B. acknowledge FAPESP, Fundação de Amparo à Pesquisa do Estado do Rio de Janeiro (FAPERJ), Coordenação de Aperfeiçoamento de Pessoal de Nível Superior (CAPES) and Conselho Nacional de Desenvolvimento Científico e Tecnológico (CNPq), for PhD and research fellowships.

References

1. Whitehouse, P. J.; Price, D. L.; Struble, R. G.; Clark, A. W.; Coyle, J. T.; DeLong, M. R.; *Science* **1982**, *215*, 1237.
2. Blennow, K.; de Leon, M. J.; Zetterberg, H.; *Lancet* **2006**, *368*, 387.
3. Ferri, C. P.; Prince, M.; Brayne, C.; Brodaty, H.; Fratiglioni, L.; Ganguli, M.; Hall, K.; Hasegawa, K.; Hendrie, H.; Huang, Y.; Jorm, A.; Mathers, C.; Menezes, P. R.; Rimmer, E.; Scazufca, M.; *Lancet* **2005**, *366*, 2112.
4. Brufani, M.; Filocampo, L.; Lappa, S.; Maggi, A.; *Drugs Future* **1997**, *22*, 397.
5. Sugimoto, H.; *Chem. Rec.* **2001**, *1*, 63.
6. Spencer, C. M.; Noble, S.; *Drugs Aging* **1998**, *13*, 391.
7. Sramek, J. J.; Franckiewicz, E. J.; Cutler, N. R.; *Expert Opin. Investig. Drugs* **2000**, *9*, 2393.
8. Robinson, D. M.; Keating, G. M.; *Drugs* **2006**, *66*, 1515.
9. Atta-ur-Rahman; Choudhary, M. I.; *Pure Appl. Chem.* **2001**, *73*, 555.
10. Ma, X.; Gang, D. R.; *Phytochemistry* **2008**, *69*, 2022.
11. Ge, H. M.; Zhu, C. H.; Shi, D. H.; Zhang, L. D.; Xie, D. Q.; Yang, J.; Ng, S. W.; Tan, R. X.; *Chem.-Eur. J.* **2008**, *14*, 376.
12. Mukherjee, P. K.; Kumar, V.; Mal, M.; Houghton, P. J.; *Planta Med.* **2007**, *73*, 283.
13. Rollinger, J. M.; Schuster, D.; Baier, E.; Ellmerer, E. P.; Langer, T.; Stuppner, H.; *J. Nat. Prod.* **2006**, *69*, 1341.
14. Oinonen, P. P.; Jokela, J. K.; Hatakka, A. I.; Vuorela, P. M.; *Fitoterapia* **2006**, *77*, 429.
15. Ingkaninan, K.; Temkitthawon, P.; Chuenchom, K.; Yuyaem, T.; Thongnoi, W.; *J. Ethnopharmacol.* **2003**, *89*, 261.
16. López, S.; Bastida, J.; Viladomat, F.; Codina, C.; *Life Sci.* **2002**, *71*, 2521.
17. Orhan, I.; Terzioglu, S.; Sener, B.; *Planta Med.* **2003**, *69*, 265.
18. Kim, D. K.; Lee, K.; *Arch. Pharm. Res.* **2003**, *26*, 735.
19. Viegas Jr., C.; Bolzani, V. S.; Barreiro, E. J.; Young, M. C.; Furlan, M.; Tomazela, D.; Eberlin, M. N.; *J. Nat. Prod.* **2004**, *67*, 908.
20. Viegas Jr., C.; Bolzani, V. S.; Pimentel, L. S.; Castro, N. G.; Cabral, R. F.; Costa, R. S.; Floyd, C.; Rocha, M. S.; Young, M. C.; Barreiro, E. J.; Fraga, C. A. M.; *Bioorg. Med. Chem.* **2005**, *13*, 4184.
21. Castro, N. G.; Costa, R. S.; Pimentel, L. S.; Danuello, A.; Romeiro, N. C.; Viegas Jr., C.; Barreiro, E. J.; Fraga, C. A. M.; Bolzani, V. S.; Rocha, M. S.; *Eur. J. Pharmacol.* **2008**, *580*, 339.
22. Pivatto, M.; Crotti, A. E. M.; Lopes, N. P.; Castro-Gamboa, I.; Rezende, A.; Viegas Jr., C.; Young, M. C. M.; Furlan, M.; Bolzani, V. S.; *J. Braz. Chem. Soc.* **2005**, *16*, 1431.

23. Raves, M. L.; Harel, M.; Pang, Y. P.; Silman, I.; Kozikowski, A. P.; Sussman, J. L.; *Nat. Struct. Biol.* **1997**, *4*, 57.
24. Harel, M.; Schalk, I.; Ehret-Sabatier, L.; Bouet, F.; Goeldner, M.; Hirth, C.; Axelsen, P. H.; Silman, I.; Sussman, J. L.; *Proc. Natl. Acad. Sci. U. S. A*. **1993**, *90*, 9031.
25. Kryger, G.; Silman, I.; Sussman, J. L.; *Struct. Fold. Des.* **1999**, *7*, 297.
26. Jia, P.; Sheng, R.; Zhang, J.; Fang, L.; He, Q.; Yang, B.; Hu, Y.; *Eur. J. Med. Chem.* **2009**, *44*, 772.
27. Bembenek, S. D.; Keith, J. M.; Letavic, M. A.; Apodaca, R.; Barbier, A. J.; Dvorak, L.; Aluisio, L.; Miller, K. L.; Lovenberg, T. W.; Carruthers, N. I.; *Bioorg. Med. Chem.* **2008**, *16*, 2968.
28. Sauvaître ,T.; Barlier, M.; Herlem, D.; Gresh, N.; Chiaroni, A.; Guenard, D.; Guillou, C.; *J. Med. Chem.* **2007**, *50*, 5311.
29. da Silva, C. H.; Carvalho, I.; Taft, C. A.; *J. Biomol. Struct. Dyn.* **2007**, *24*, 515.
30. Correa-Basurto, J.; Flores-Sandoval, C.; Marín-Cruz, J.; Rojo-Domínguez, A.; Espinoza-Fonseca, L. M.; Trujillo-Ferrara, J. G.; *Eur. J. Med. Chem.* **2007**, *42*, 10.
31. Rarey, M.; Kramer, B.; Lengauer, T.; Klebe, G.; *J. Mol. Biol.* **1996**, *261*, 470.
32. Clauben , H.; Buning, C.; Rarey, M.; Lengauer, T.; *J. Mol. Biol.* **2001**, *308*, 377.
33. Gasteiger , J.; Marsili, M.; *Tetrahedron* **1980**, *36*, 3219.
34. Berman, H. M.; Westbrook, J.; Feng, Z.; Gilliland, G.; Bhat, T. N.; Weissig, H.; Shindyalov, I. N.; Bourne, P. E.; *Nucleic Acids Res.* **2000**, *28*, 235.
35. Cornell, W. D.; Cieplak, P.; Bayly, C. I.; Gould, I. R.; Merz Jr., K. M.; Ferguson, D. M.; Spellmeyer, D. C.; Fox, T.; Caldwell, J. W.; Kollman, P. A.; *J. Am. Chem. Soc.* **1995**, *117*, 5179.
36. van Aalten, D. M. F.; Bywater, B.; Findlay, J. B. C.; Hendlich, M.; Hooft, R. W. W.; Vriend, G.; *J. Comput. Aided Mol. Des.* **1996**, *10*, 255.
37. Schmidt , M. W; Baldridge, K. K.; Boatz, J. A.; Elbert, S. T.; Gordon, M. S.; Jensen, J. H.; Koseki, S.; Matsunaga, N.; Nguyen, K. A.; Su, S. J.; Windus, T. L.; Dupuis, M.; Montgomery, J. A.; *J. Comput. Chem.* **1993**, *14*, 1347.
38. Berendsen, H. J. C.; van der Spoel, D.; van Drunen, R.; *Comput. Phys. Commun.* **1995**, *91*, 43.
39. Verli, H.; Guimarães, J. A.; *Carbohydr. Res.* **2004**, *339*, 281.
40. Becker, C. F.; Guimarães, J. A.; Mourão, P. A. S.; Verli, H.; *J. Mol. Graphics Modell.* **2007**, *26*, 391.
41. Verli, H.; Guimarães, J. A.; *J. Mol. Graphics Modell.* **2005**, *24*, 203.
42. Groot, B. L.; Grubmüller, H.; *Science* **2001**, *294*, 2353.
43. Berendsen, H. J. C.; Grigera, J. R.; Straatsma, T. P.; *J. Phys. Chem.* **1987**, *91*, 6269.
44. Hess, B.; Bekker, H.; Berendsen, H. J. C.; Fraaije, J. G. E. M.; *J. Comput. Chem.* **1997**, *18*, 1463.
45. Darden, T.; York, D.; Pedersen, L.; *J. Chem. Phys.* **1993**, *98*, 10089.
46. Berendsen, H. J. C.; Postma, J. P. M.; DiNola, A.; Haak, J. R.; *J. Chem. Phys.* **1984**, *81*, 3684.
47. Theodorsson-Norheim, E.; *Comput. Methods Programs Biomed.* **1986**, *23*, 57.
48. Tukey, J. W.; Ciminera, J. L.; Heyse, J. F.; *Biometrics* **1985**, *41*, 295.
49. Wilcoxon, F.; *J. Econ. Entomol.* **1946**, *39*, 269.
50. Mann, H. B.; Whitney, D. R.; *Ann. Math. Statist.* **1947**, *18*, 50.

Submitted: May 5, 2011
Published online: December 1, 2011

FAPESP has sponsored the publication of this article.

J. Braz. Chem. Soc., Vol. 00, No. 00, S1-S4, 2011.
Printed in Brazil - ©2011 Sociedade Brasileira de Química
0103 - 5053 $6.00+0.00

Supplementary Information

Molecular Docking and Molecular Dynamic Studies of Semi-Synthetic Piperidine Alkaloids as Acetylcholinesterase Inhibitors

Amanda Danuello,[a] Nelilma C. Romeiro,[b] Guilherme M. Giesel,[c] Marcos Pivatto,[a] Claudio Viegas Jr.,[d] Hugo Verli,[c,e] Eliezer J. Barreiro,[b] Carlos A. M. Fraga,[b] Newton G. Castro[f] and Vanderlan S. Bolzani*[,a]

[a]Núcleo de Bioensaios, Biossíntese e Ecofisiologia de Produtos Naturais (NuBBE), Departamento de Química Orgânica, Instituto de Química, Universidade Estadual Paulista 'Julio de Mesquita Filho', CP 355, 14801-970 Araraquara-SP, Brazil

[b]Laboratório de Avaliação e Síntese de Substâncias Bioativas (LASSBio), Faculdade de Farmácia, Universidade Federal do Rio de Janeiro, CP 68023, 21944-910 Rio de Janeiro-RJ, Brazil

[c]Centro de Biotecnologia, Universidade Federal do Rio Grande do Sul, Av. Bento Gonçalves 9500, CP 15005, 91500-970 Porto Alegre-RS, Brazil

[d]Laboratório de Fitoquímica e Química Medicinal (LFQM), Departamento de Ciências Exatas, Universidade Federal de Alfenas, 37130-000 Alfenas-MG, Brazil

[e]Faculdade de Farmácia, Universidade Federal do Rio Grande do Sul, Av. Ipiranga 2752, 90610-000 Porto Alegre- RS, Brazil

[f]Departamento de Farmacologia Básica e Clínica, Instituto de Ciências Biomédicas, Universidade Federal do Rio de Janeiro, CCS Bloco J Sala J1-029, 21941-902 Rio de Janeiro-RJ, Brazil

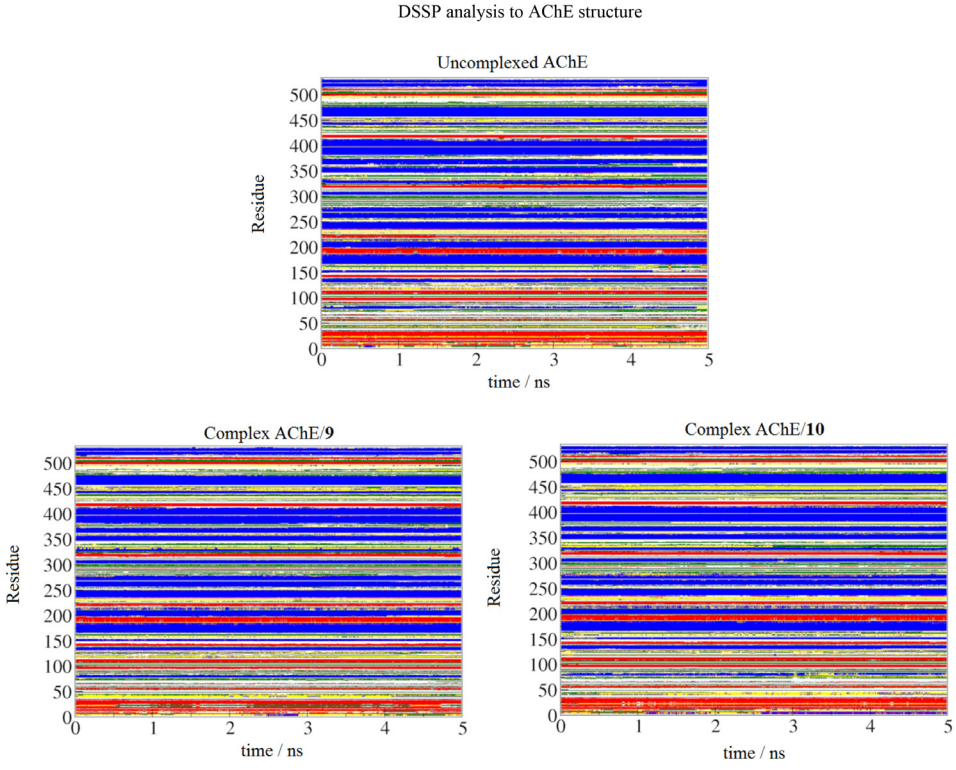

Figure S1. DSSP analysis describing the content of the secondary structure of AChE as a function of simulation time. Coils are represented in white, β-sheets in red, β-bridges in black, bends in green, turns in yellow, α-helix in blue and 3_{10}-helix in grey.

*e-mail: bolzaniv@iq.unesp.br

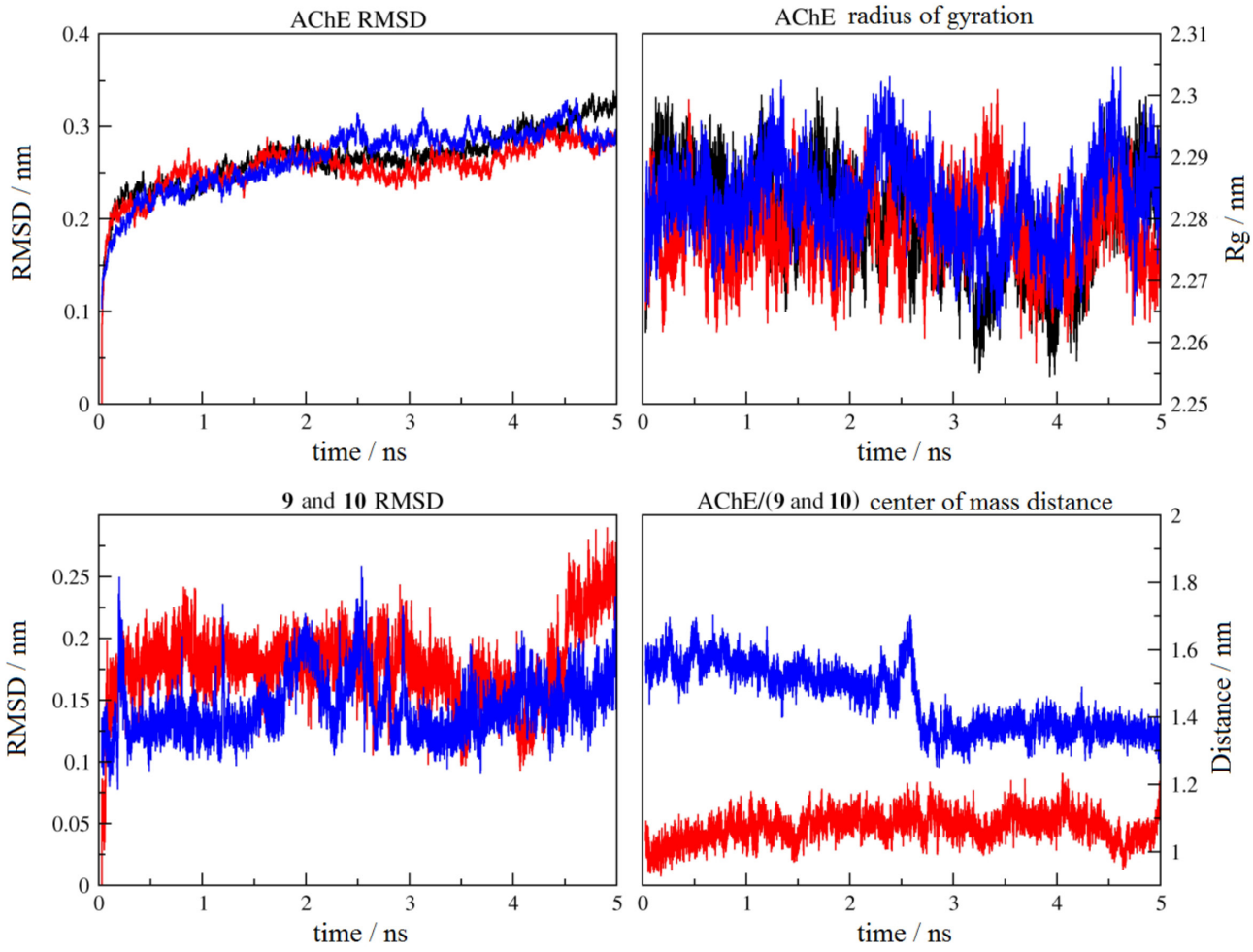

Figure S2. Characterization of the dynamic behavior of the performed simulations, including root mean square deviation (RMSD), radius of gyration, and center of mass distance between compounds **9** and **10** and the protein. Black curves represent uncomplexed AChE, red curves correspond to the AChE/**9** complex and the AChE/**10** complex is shown in blue.

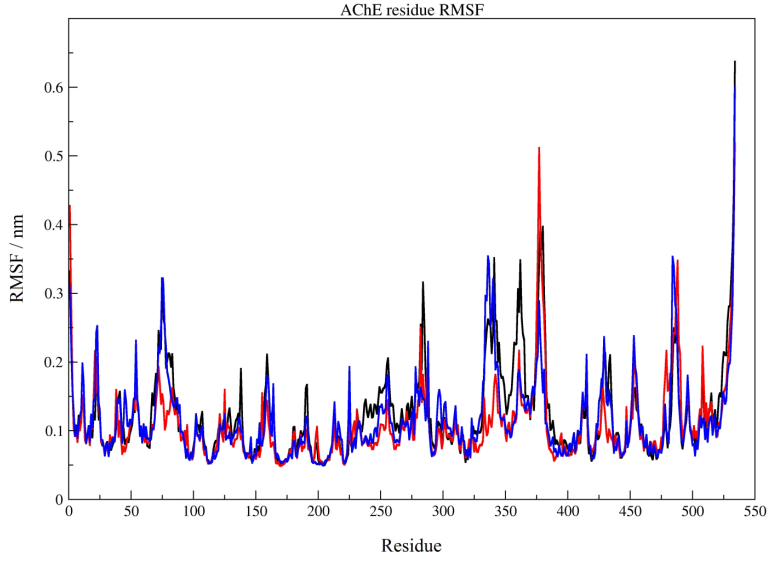

Figure S3. Root mean square fluctuation (RMSF) for AChE residues considering the entire simulation. Black curve represents uncomplexed AChE, red curve displays the AChE/**9** complex and the blue curve corresponds to the AChE/**10** complex.

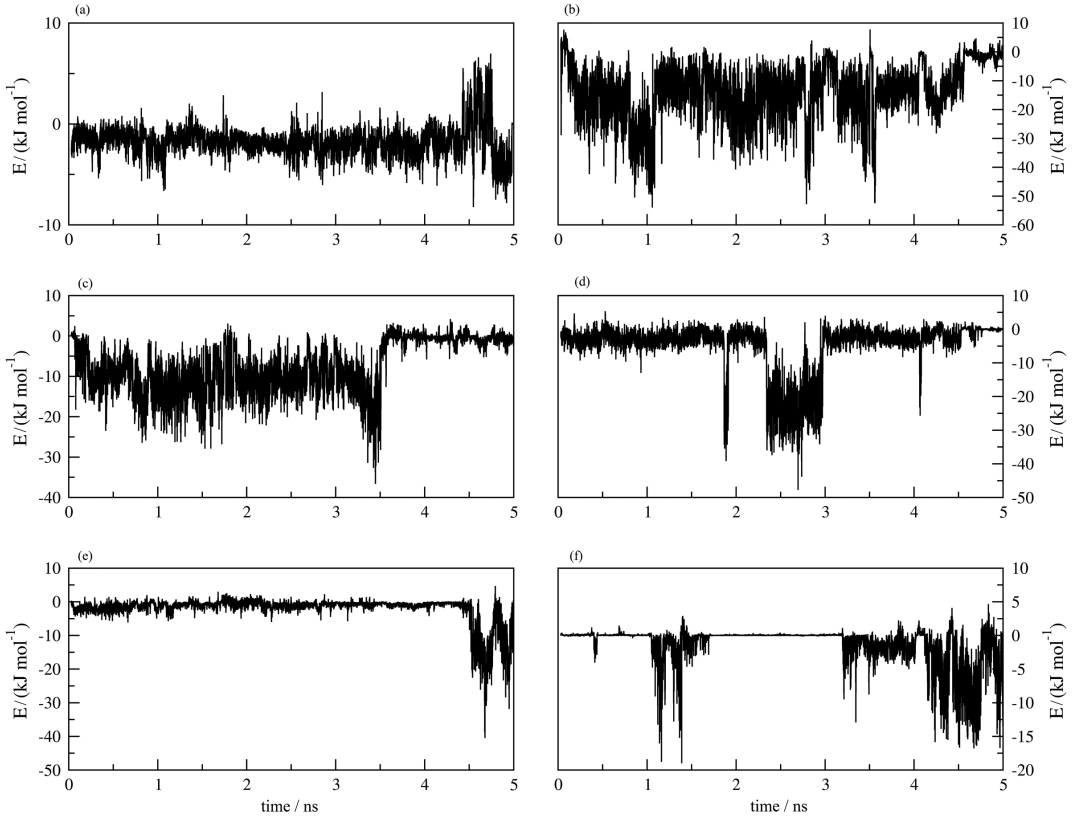

Figure S4. Interaction energy fluctuation along the MD simulation between **9** and AChE residues: (a) Tyr70, (b) Asp72, (c) Trp84, (d) Tyr121, (e) Ser122 and (f) Trp432.

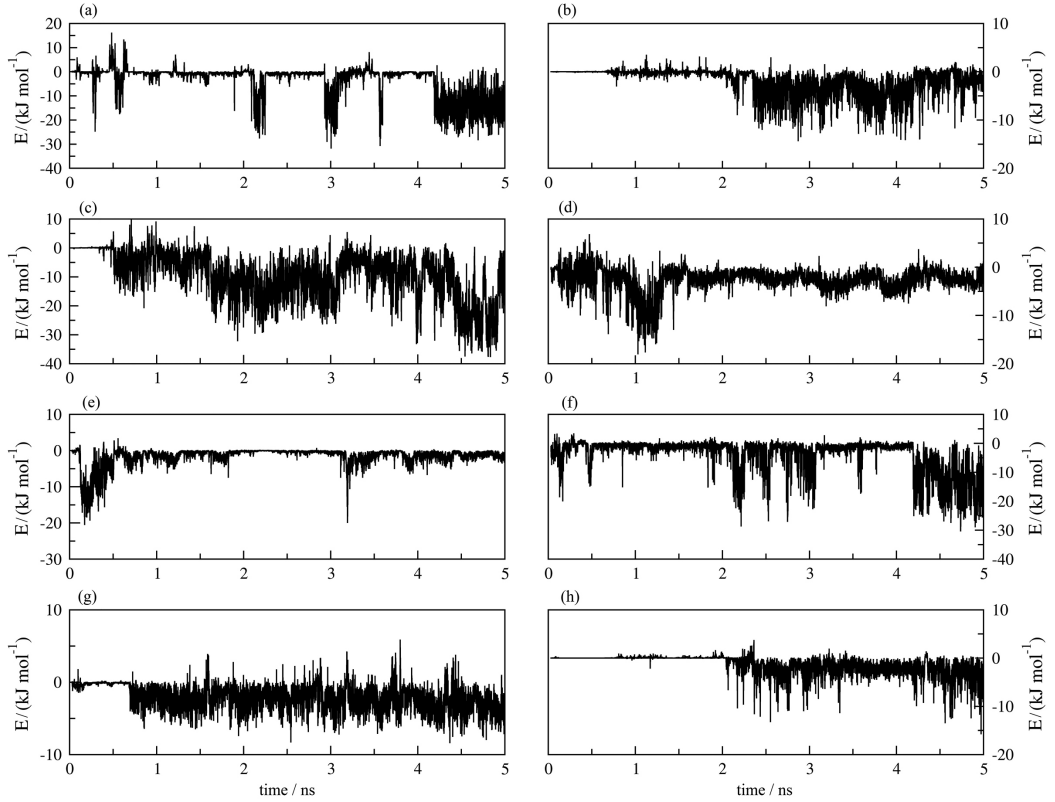

Figure S5. Interaction energies fluctuation along the MD simulation between **10** and AChE residues: (a) Gln74, (b) Trp84, (c) Asp285, (d) Ser286, (e) Arg289, (f) Tyr334, (g) Gly335 and (h) Trp432.

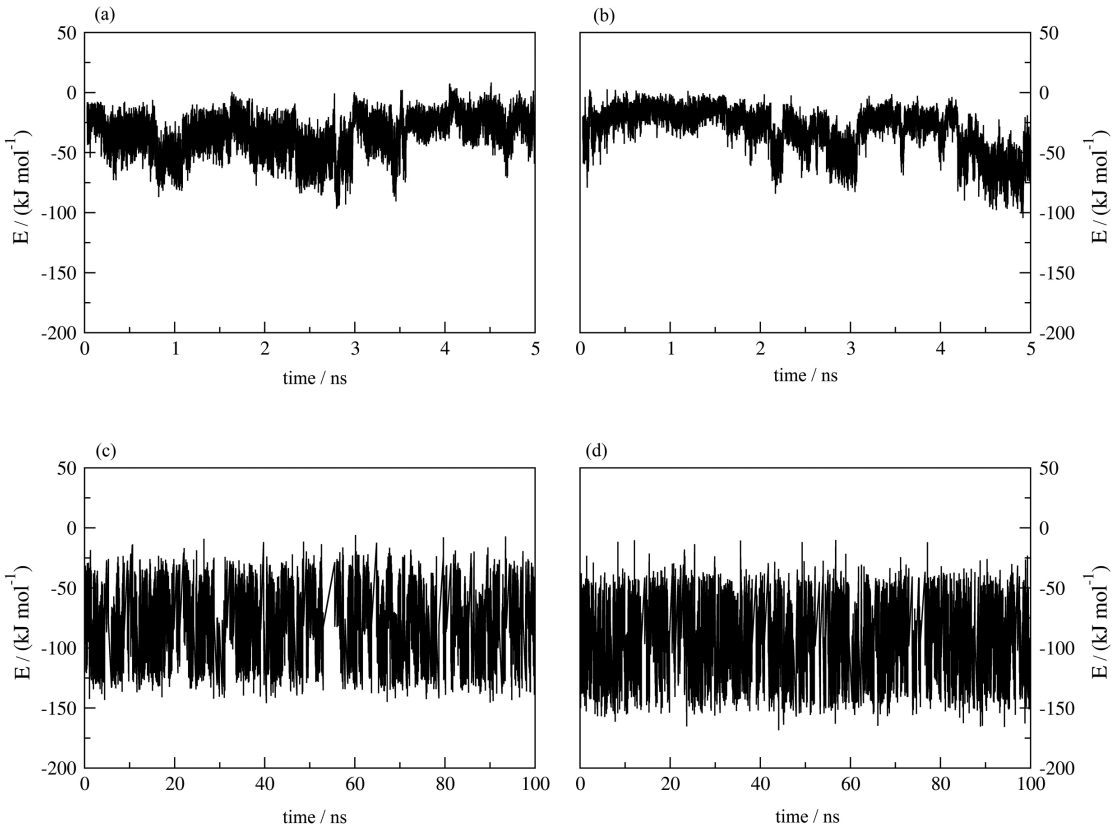

Figure S6. Total interaction energy fluctuation along the MD simulation: (a) **9** – AChE interaction, (b) **10** – AChE interaction, (c) **9** – solvent interaction and (d) **10** – solvent interaction.

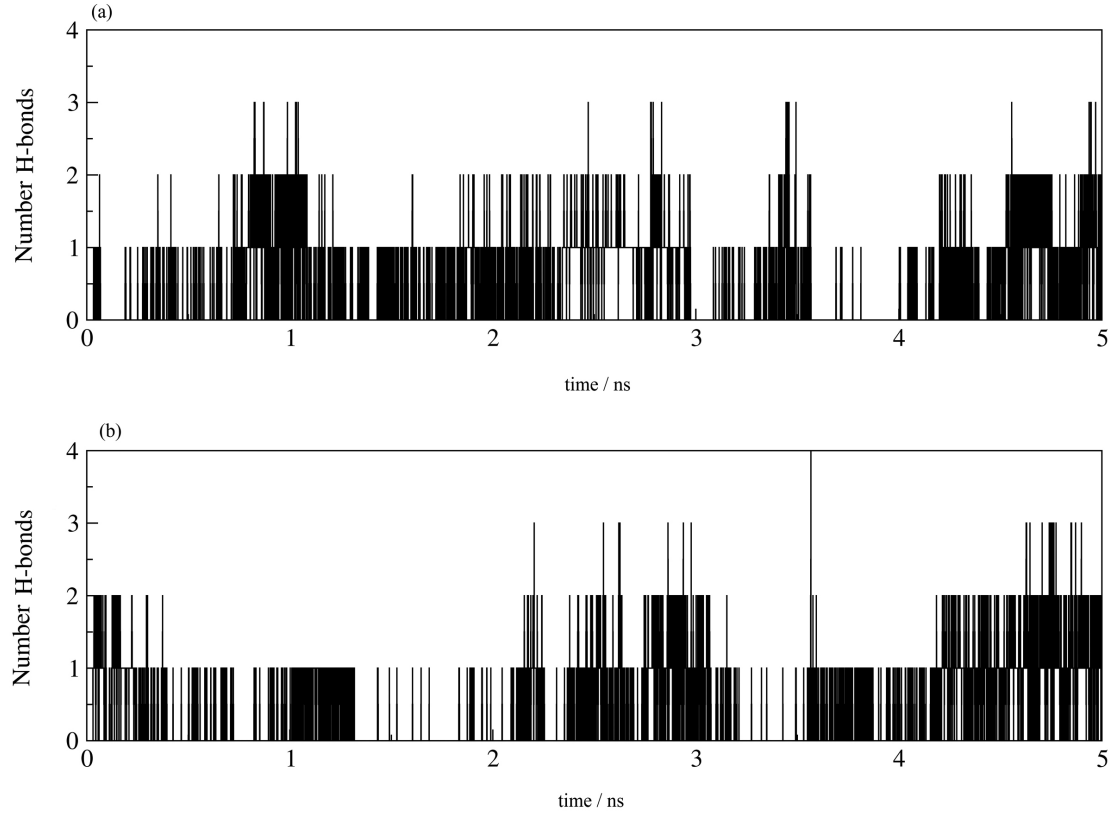

Figure S7. Evaluation of the total number of H-bonds established between the studied ligands and AChE along the MD simulation: (a) AChE/**9** complex and (b) AChE/**10** complex.